JOURNAL OF GEOPHYSICAL RESEARCH, VOL. 112, D12305, doi:10.1029/2006JD008268, 2007

Atmospheric acetylene and its relationship with CO as an indicator of air mass age

Yaping Xiao,[1,2] Daniel J. Jacob,[1] and Solene Turquety[1,3]

Received 20 November 2006; revised 12 February 2007; accepted 5 March 2007; published 21 June 2007.

[1] Acetylene (C_2H_2) and CO originating from combustion are strongly correlated in atmospheric observations, offering constraints on atmospheric dilution and chemical aging. We examine here the C_2H_2-CO relationships in aircraft observations worldwide, and interpret them with simple models as well as with a global chemical transport model (GEOS-Chem). A C_2H_2 global source of 6.6 Tg yr^{-1} in GEOS-Chem simulates the ensemble of global C_2H_2 observations without systematic bias, and captures most seasonal and regional features. C_2H_2/CO concentration ratios decrease from continental source regions to the remote atmosphere in a manner consistent between the observations and the model. However, the dC_2H_2/dCO slope from the linear regression does not show such a systematic decrease, either in the model or in the observations, reflecting variability in background air. The slope $\beta = d\log[C_2H_2]/d\log[CO]$ of the linear regression of concentrations in log space offers information for separating the influences of dilution and chemical aging. We find that a linear mixing model with constant dilution rate and background is successful in fresh continental outflow but not in remote air. A diffusion model provides a better conceptual framework for interpreting the observations, where the value of β relative to the square root of the ratio of C_2H_2 and CO chemical lifetimes (1.7–1.9) measures the relative importance of dilution and chemistry. We thus find that dilution dominates in fresh outflow but chemical loss dominates in remote air. This result is supported by GEOS-Chem sensitivity simulations with modified OH concentrations, and suggests that the model overestimates OH in the southern tropics.

Citation: Xiao, Y., D. J. Jacob, and S. Turquety (2007), Atmospheric acetylene and its relationship with CO as an indicator of air mass age, *J. Geophys. Res.*, *112*, D12305, doi:10.1029/2006JD008268.

1. Introduction

[2] Acetylene (C_2H_2) and carbon monoxide (CO) have common sources from combustion and are highly correlated in atmospheric observations [*Blake et al.*, 1992, 1993, 1999, 2001, 2003; *Wofsy et al.*, 1992; *Wang et al.*, 2003]. They are both removed from the atmosphere by reaction with the OH radical, with mean lifetimes of about two weeks for C_2H_2 and 2 months for CO. A number of studies have used the observed C_2H_2/CO concentration ratio as a tracer of the age of air since it last encountered a combustion source region [*Smyth et al.*, 1996; *Gregory et al.*, 1997; *Russo et al.*, 2003; *Swanson et al.*, 2003], following the general use for this purpose of hydrocarbon pairs with common sources and different lifetimes [*Parrish et al.*, 1992; *McKeen and Liu*, 1993; *Parrish et al.*, 2004; *de Gouw et al.*, 2005]. The C_2H_2-CO pair is of particular value for diagnosing the age of air in the remote troposphere because the C_2H_2 lifetime is long and the observed correlation with CO remains strong. Beyond its qualitative use as a tracer of the age of air, the C_2H_2-CO relationship may offer important quantitative information to test our understanding of OH levels and global atmospheric dilution rates.

[3] *McKeen et al.* [1996] offered the first theoretical analysis for interpreting relationships between hydrocarbon pairs in terms of relative contributions of dilution and chemical aging. They treated the transport term as a linear mixing between the point of emission and a uniform background, and showed that dilution with nonzero background complicates the simple interpretation of log-log concentration relationships as a measure of chemical aging ("photochemical clock"). They presented an improved interpretation in terms of both chemical and dilution rate constants. The simple linear mixing assumption is acceptable in the initial stages of dilution of a large isolated source in an otherwise clean atmosphere, but it is questionable for interpreting correlations in the remote troposphere and this limitation was acknowledged by *McKeen et al.* [1996].

[4] *Ehhalt et al.* [1998] addressed this difficulty by using a hierarchy of atmospheric transport models including one-dimensional (turbulent diffusion), two-dimensional (diffusion-advection), and three-dimensional to examine the information content of correlations between idealized

[1]Department of Earth and Planetary Sciences and Division of Engineering and Applied Sciences, Harvard University, Cambridge, Massachusetts, USA.
[2]Now at Climate Change Research Center, University of New Hampshire, Durham, New Hampshire, USA.
[3]Now at Service d'Aéronomie, IPSL, Paris, France.

0148-0227/07/2006JD008268$09.00

chemical tracers with fixed lifetimes and common continental emissions. They found that the log-log concentration relationship for a pair of tracers varies with the model representation of transport. In the three-dimensional model, the slope of the log-log regression line typically varied between 1 (aging controlled by dilution) and the square root of the ratio of chemical lifetimes (comparable contributions from dilution and chemical decay), but could also be higher (aging dominated by chemical decay).

[5] In this paper, we analyze the variability of the C_2H_2-CO relationships for a large ensemble of aircraft observations in different regions of the world, and examine the validity of the *McKeen et al.* [1996] and *Ehhalt et al.* [1998] conceptual models for interpreting these relationships. We also apply a global chemical transport model (GEOS-Chem CTM) to interpret the observed C_2H_2-CO relationships in different parts of the world and use them as a test of model transport and chemical processes.

[6] An important first step in our analysis is to construct a global atmospheric budget for C_2H_2. Previous estimates vary over a wide range. *Gupta et al.* [1998] estimated a global C_2H_2 emission of 3.1 Tg yr^{-1} as the needed flux boundary condition for a two-dimensional simulation of C_2H_2 constrained with atmospheric observations at remote sites. The Emission Database for Global Atmospheric Research (EDGAR) for 1990 [*Olivier et al.*, 1996] gives C_2H_2 emission totals of 1.7, 1.2, and 1.7 Tg yr^{-1} from fossil fuel, biofuel, and biomass burning. *Gautrois et al.* [2003] found that the EDGAR inventory for 1990 had to be scaled up by more than a factor of 2 in the extratropical Northern Hemisphere to match the C_2H_2 observations at the Alert site in the Canadian Arctic. *Kanakidou et al.* [1988] and *Plass-Dulmer et al.* [1995] identified a small oceanic source (0.2–1.4 Tg yr^{-1}) that could significantly affect the interpretation of C_2H_2-CO correlations in remote oceanic air. We use here a GEOS-Chem simulation of C_2H_2 observations worldwide, together with observations of C_2H_2/CO enhancement ratios in source regions, to better constrain the global C_2H_2 source and its distribution.

2. Model Description

2.1. General Description

[7] We use the GEOS-Chem global three-dimensional CTM (version 5.04) driven by assimilated meteorological observations from the NASA Goddard Earth Observing System (GEOS) [*Bey et al.*, 2001]. Our analysis is based on a 1-year simulation of C_2H_2 and CO for 2001, starting in July 2000 to ensure proper initialization. The GEOS-3 meteorological fields for 2001 have $1^\circ \times 1^\circ$ horizontal resolution, 48 layers in the vertical, and 6-hour temporal resolution (3-hour for mixing depths and surface properties). For computational expediency we degrade the horizontal resolution in GEOS-Chem to 2° latitude $\times$ 2.5° longitude. The simulation of transport includes a flux form semi-Lagrangian advection scheme applied to the grid-scale winds [*Lin and Rood*, 1996], a Relaxed Arakawa-Schubert convection scheme [*Moorthi and Suarez*, 1992] using archived convective mass fluxes, and full vertical mixing within the GEOS-diagnosed mixing depth generated by surface instability. We also conduct shorter simulations using 1996 (GEOS-Strat) and 2004 (GEOS-4) meteorological fields for analysis of the PEM-Tropics A and INTEX-A aircraft data sets, as discussed further below.

[8] Sources of C_2H_2 and CO are described in section 2.2. Reaction with OH is the only significant atmospheric sink for C_2H_2 and CO, and the corresponding rate constants are from *DeMore et al.* [1997]. Reaction of C_2H_2 with OH is a three-body reaction but has only weak sensitivity to temperature or pressure. The rate constant decreases by about 20% when temperature decreases from 300 to 270 K or when the pressure decreases from 1000 to 500 hPa. Reactions of C_2H_2 with O_3 and NO_3 are negligibly slow [*Atkinson*, 2000]. We compute chemical loss of C_2H_2 and CO with archived monthly mean three-dimensional OH concentrations from a GEOS-Chem (version 4.33) simulation of tropospheric ozone-NO_x-hydrocarbon chemistry [*Fiore et al.*, 2003]. The resulting global mean tropospheric lifetimes are 12 days for C_2H_2 and 60 days for CO. A standard test for the global mean OH concentration computed in a CTM is the tropospheric lifetime of methylchloroform, which should be in the range 5.3–6.9 years as constrained by observed atmospheric concentrations and emission inventories [*Prinn et al.*, 2001]. The *Fiore et al.* [2003] OH fields yield a lifetime of 6.3 years, consistent with that constraint.

2.2. Sources of C_2H_2 and CO

[9] Table 1 shows the combustion sources of C_2H_2 and CO used in the model. Sources of CO are as described by Duncan et al. (B.N. Duncan et al., The global budget of CO, 1988–1997: Source estimates and validation with a global model, submitted to *Journal of Geophysical Research*, 2006) and include 480 Tg yr^{-1} from fossil fuel, 190 Tg yr^{-1} from biofuel, and 490 Tg yr^{-1} from climatological biomass burning. These numbers include direct CO emission plus the chemical source from oxidation of short-lived hydrocarbons coemitted from combustion. The chemical source amounts to 18% of direct CO emission for fossil fuel and biofuel, and 11% for biomass burning. The fossil fuel and biofuel sources are aseasonal. The biomass burning source has monthly temporal variation specified from multiyear satellite data [*Duncan et al.*, 2003]. The GEOS-Chem CO simulation has been evaluated extensively with observations in the work of Duncan et al. (hereinafter referred to as Duncan et al., submitted manuscript, 2006) and other studies [*Heald et al.*, 2003, 2004; *Jaeglé et al.*, 2003; *Palmer et al.*, 2003; *Duncan and Bey*, 2004; *Liang et al.*, 2004]. It is overall unbiased in the Northern Hemisphere relative to MOPITT satellite observations [*Heald et al.*, 2003].

[10] Simulation of the INTEX-A aircraft data over North America in summer 2004 uses a modified regional CO source inventory as needed to match the constraints from the aircraft and MOPITT observations [*Hudman et al.*, 2007; *Turquety et al.*, 2007]. The US fossil fuel source of CO is 5.0 Tg yr^{-1}, as compared to 7.3 Tg yr^{-1} by Duncan et al. (hereinafter referred to as Duncan et al., submitted manuscript, 2006) reflecting recent emission decreases [*Parrish*, 2006; *Hudman et al.*, 2007]. North American biomass burning for summer 2004 is simulated with a daily emission inventory that accounts for large Alaskan and Canadian fires during that period and pyroconvective injection to the free troposphere [*Turquety et al.*, 2007].

[11] Our fossil fuel source of C_2H_2 is based on the EDGAR inventory for 1990 with $1^\circ \times 1^\circ$ horizontal

Table 1. Global Combustion Source Inventories for C_2H_2 and CO

	Fossil Fuel	Biofuel	Biomass Burning
C_2H_2, Tg yr^{-1}	1.7	3.3	1.6
CO, 10^3 Tg yr^{-1}	0.48	0.19	0.49
C_2H_2/CO[a], 10^{-3} mol mol^{-1}	4.8 (East Asia)[b]	19	3.6
	2.5 (elsewhere) (2–11)[c]	(5–21)[d]	(2–4.5)[e]

[a]C_2H_2/CO combustion source ratios in the model. Numbers in parentheses are literature ranges.
[b]From *Streets et al.* [2003].
[c]From *Sigsby et al.* [1987], *Pierson et al.* [1996], *Grosjean et al.* [1998], and *Harley et al.* [2001].
[d]From *Bertschi et al.* [2003].
[e]From *Hegg et al.* [1990] and *Blake et al.* [1996].

resolution and no seasonal variation [*Olivier et al.*, 1996]; 90% of that source is from transportation. For the United States, EDGAR gives an emission total of 0.26 Tg yr^{-1}, as compared to 0.079 Tg yr^{-1} in the National Emission Inventory for 1999 (NEI-99) of the US Environmental Protection Agency (EPA). Underestimate of C_2H_2 emissions in NEI-99 has been previously pointed out by *Fortin et al.* [2005]. For East Asian C_2H_2 emissions, we adopt the spatial distribution of EDGAR but scale the total to that of *Streets et al.* [2003], which gives a regional total of 0.91 Tg yr^{-1} as compared to 0.25 Tg yr^{-1} in EDGAR. The *Streets et al.* [2003] estimate is more consistent with Asian outflow observations from the TRACE-P aircraft mission [*Carmichael et al.*, 2003].

[12] The resulting C_2H_2/CO molar emission ratio for fossil fuel is 4.8×10^{-3} in East Asia and 2.5×10^{-3} elsewhere (4.6×10^{-3} for the INTEX-A conditions due to the CO emission decrease). Aircraft observations in the urban plume of Nashville, Tennessee give a C_2H_2/CO enhancement ratio of 6×10^{-3} [*Harley et al.*, 2001]. A much higher ratio of 11.4×10^{-3} was observed by *Grosjean et al.* [1998] for urban air in Brazil. Canister measurements from 43 Chinese cities indicate a mean ratio of 5×10^{-3} [*Barletta et al.*, 2005], while observations of the fresh Shanghai plume during TRACE-P show a maximum ratio of 9.4×10^{-3} [*Russo et al.*, 2003]. Variability in the C_2H_2/CO emission ratio from vehicles could reflect the use and condition of catalysts [*Sigsby et al.*, 1987].

[13] We estimate the biomass burning source of C_2H_2 by applying a C_2H_2/CO molar emission ratio of 4×10^{-3} [*Andreae and Merlet*, 2001] to the biomass burning source of CO. Literature on C_2H_2/CO molar emission ratios from biomass burning include $2–4 \times 10^{-3}$ for seven forest fires in North America [*Hegg et al.*, 1990], and $3.3–4.5 \times 10^{-3}$ for Brazilian and African fires sampled in the TRACE-A aircraft campaign [*Blake et al.*, 1996; *Hao et al*, 1996].

[14] Biofuel emissions of C_2H_2 are estimated by applying a molar ratio of 19×10^{-3} to the corresponding source of CO. This high emission ratio is based on the measurements by *Bertschi et al.* [2003], which are to our knowledge the only available. *Bertschi et al.* [2003] also find high emission ratios relative to biomass burning for other compounds including C_2H_6, organic acids, and NH_3, and this may relate to the flaming combustion character of biofuel fires [*Yokelson et al.*, 2003]. The Asian regional total C_2H_2 emission from biofuel is 1.7 Tg yr^{-1}, as compared to 1.3 Tg yr^{-1} in the work of *Streets et al.* [2003].

Table 2. C_2H_2 Measurements Used for Model Evaluation

	Observation Period	Reference
Surface Stations		
Arctic		
Alert (82°N,63°W)	1989–1996	*Gautrois et al.* [2003]
Zeppelin (78°N, 11°E), 474 m	Sep. 1989–Dec. 1994	*Solberg et al.* [1996]
Europe		
Pallas (68°N, 24°E)	Jan. 1994–Dec. 1994	*Laurila and Hakola* [1996]
Uto (60°N, 21°E)	Jan. 1993–Dec. 1994	*Laurila and Hakola* [1996]
Rorvik (57°N, 12°E)	Feb. 1989–Oct. 1990	*Laurila and Hakola* [1996]
Birkenes (58°N, 8°E)	Jan. 1988–Dec. 1994	*Solberg et al.* [1996]
Rucava (56°N, 21°E)	Sep. 1992–Dec. 1994	*Solberg et al.* [1996]
Waldhof (52°N, 10°E)	Oct. 1992–Dec. 1994	*Solberg et al.* [1996]
Kosetice (49°N, 15°E)	Aug. 1992–Dec. 1994	*Solberg et al.* [1996]
Tanikon (47°N, 8°E)	Sep. 1992–Dec. 1994	*Solberg et al.* [1996]
North America		
Harvard Forest (43°N, 72°W)	1992–1994	*Goldstein et al.* [1995]
Ground-Based Column Stations[a]		
Spitsbergen (79°N, 12°E)	1992–1999	*Notholt et al.* [1997]
Jungfraujoch (47°N, 8°E), 3.6 km	1986–2000	*Mahieu et al.* [1997]
Japan (44°N, 143°E)[b]	May 1995–Jun. 2000	*Zhao et al.* [2002]
Aircraft Missions		
1. TRACE-P, China Coast (25°–40°N, 122°–126°E)	Feb.–Apr. 2001	*Jacob et al.* [2003]
2. TRACE-P, west tropical Pacific (13°–25°N, 126°–146°E)		
3. TRACE-P, northeastern tropical Pacific (15°–35°N, 120°–160°W)		
4. PEM-West A, northwestern Pacific (20–50°N, 120°–150°E)	Sep.–Oct. 1991	*Hoell et al.* [1996]
5. PEM-Tropics B, southern tropical Pacific (10°–30°S, 160°E–100°W)	Mar.–Apr. 1999	*Raper et al.* [2001]
6. PEM-Tropics A, southern tropical Pacific (10°–35°S, 170°E–145°W)	Aug.–Sep. 1996	*Hoell et al.* [1999]
7. TRACE-A, South Africa (0°–20°S, 0°–10°E)	Sep.–Oct. 1992	*Fishman et al.* [1996]
8. INTEX-A, North America (28°–50°N, 55°–95°W)	Jul.–Aug. 2004	*Singh et al.* [2006]
9. North Atlantic Ocean (55°–58°N, 5°–10°W)[c]	Jan. 1987–Apr. 1990	*Penkett et al.* [1993]

[a]Sensitivity of the retrieval to atmospheric concentrations (averaging kernel) is within 10% of unity at all altitudes (Justus Notholt, personal communication). A sensitivity of unity is assumed in the comparison to model results, so that the model values in Figure 3 are actual columns.
[b]Average of observations at Moshiri (44.4°N, 142.3°E) and Rikubetsu (43.5°N, 143.8°E).
[c]These C_2H_2 observations are in near-surface air and are used in the surface site evaluation (Figure 2). No CO observations were made.

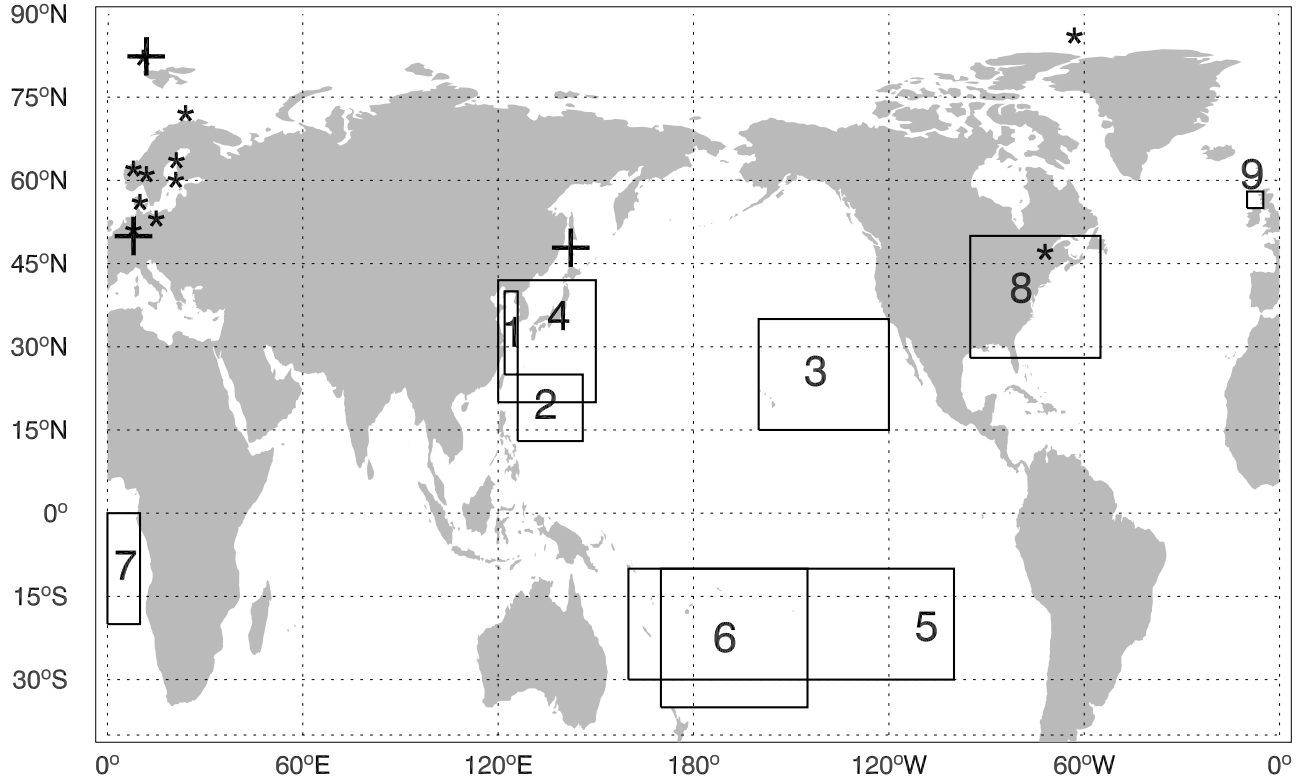

Figure 1. C_2H_2 observations (see Table 2) used for model evaluation. Stars denote surface sites. Pluses denote FTIR column stations. The boxes are sampling regions from aircraft missions.

[15] We do not include an oceanic source of C_2H_2. Observed C_2H_2 vertical profiles in the remote marine atmosphere do not show a marine boundary layer enhancement [*Blake et al.*, 2001], whereas a sensitivity simulation with an oceanic source of 0.5 Tg yr^{-1} shows such an enhancement. We conclude that the oceanic source must be at the low end of the range of the estimates of *Kanakidou et al.* [1988] (0.2–1.4 Tg yr^{-1}) and *Plass-Dulmer et al.* [1995] (0.2–0.5 Tg yr^{-1}).

[16] Overall, our global C_2H_2 source is 6.6 Tg yr^{-1} (1.7 from fossil fuel, 3.3 from biofuel, 1.6 from biomass burning). Biofuel accounts for 50% of the total C_2H_2 source. Asia accounts for 70% of the biofuel source, and as we will see this is consistent with aircraft observations in Asian outflow.

3. Simulation of Acetylene: Comparison to Observations

[17] We evaluated the C_2H_2 simulation with the ensemble of observations from surface sites and aircraft missions listed in Table 2, with locations shown in Figure 1. Figures 2 and 3 show the simulated and observed C_2H_2 concentrations at the surface stations and FTIR column measurement sites (all in the extratropical Northern Hemisphere). Figure 2 also includes near-surface aircraft observations over the North Atlantic from *Penkett et al.* [1993], which provide year-round data. In general, the model reproduces the magnitudes and seasonal variations of the observations, with no significant biases. The seasonal variation is mainly driven by OH. The good agreement between model and observations implies a good representation of both C_2H_2 sources and OH concentrations in the extratropical Northern Hemisphere [*Goldstein et al.*, 1995]. An exception is Jungfraujoch, where the observations show a May maximum and winter minimum that is at odds not only with the model but also with observations at other sites. Observations at Zeppelin and Spitsbergen (column) suggest that the model is too high in Arctic winter, but this bias is not apparent at Alert.

[18] Figure 4 shows simulated and observed vertical profiles of C_2H_2 concentrations from the aircraft missions of Table 2 and for the regions of Figure 1. These data cover the ensemble of 1991–2004 DC-8 aircraft missions from the NASA Global Tropospheric Experiment (GTE), with the exception of the PEM-West B mission over the NW Pacific in February–March 1994 because of geographical and seasonal overlap with the TRACE-P mission. Our model simulation is for the same year as TRACE-P [2001] and thus is better compared to observations from that mission than to PEM-West B. Model vertical profiles are constructed by averaging the model data sampled along the flight tracks and on the flight days for the 2001 model year, except INTEX-A (region 8) for which we use 3-hour model data for 2004, and PEM-Tropics A (region 6) for which we also show 1996 model data.

[19] The TRACE-P observations (March–April 2001) over the NW Pacific north of 30°N are heavily affected by boundary layer outflow from China [*Liu et al.*, 2003]. The vertical profile over the China coast (region 1) shows a large boundary layer enhancement that is reproduced by the model, supporting the magnitude of the Asian source

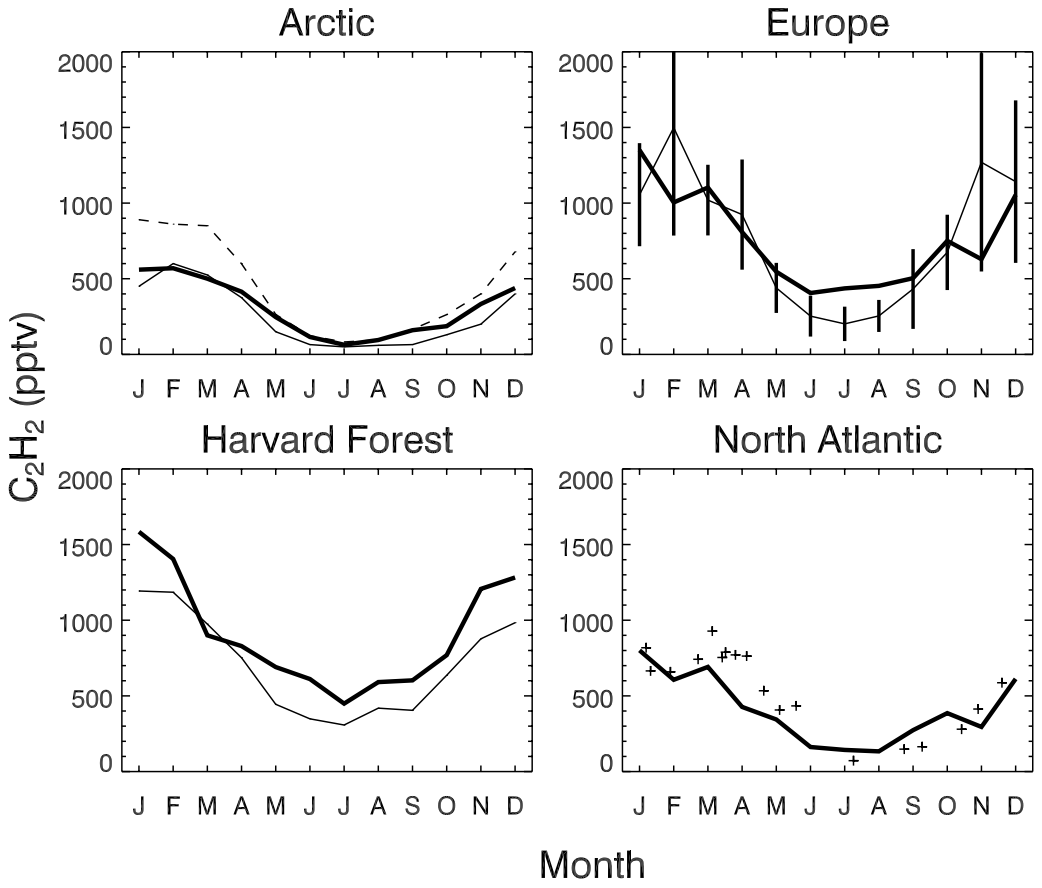

Figure 2. Simulated (thick lines) and observed (thin lines) C_2H_2 concentrations at the sites of Table 2. Observations are multiyear records and are averaged over all measurement years. Arctic observations are for Alert (solid) and Zeppelin (dashed), The European observations are shown as monthly median values and standard deviations for all sites in Table 2. The North Atlantic observations (+) are aircraft measurements in near-surface air from *Penkett et al.* [1993]. Model values are monthly means averaged over the observing stations.

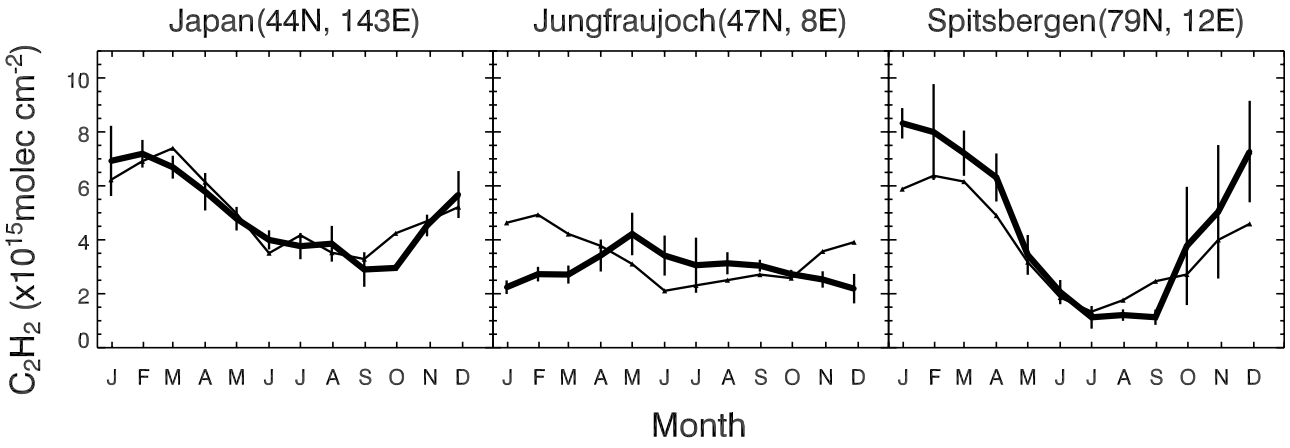

Figure 3. Simulated (thin lines) and observed (thick lines) C_2H_2 columns at Moshiri&Rikubetsu in Japan, Jungfraujoch in the Swiss Alps at 3.6 km altitude, and Ny Alesund in Spitsbergen. Values are monthly means. Observations are from multiyear records (Table 2) and are averaged over all measurement years. Vertical bars are standard deviations describing the interannual variability in the monthly mean data. Observations between September 1997 and September 1998 have been excluded because of anomalous fire influence [*Rinsland et al.*, 1999].

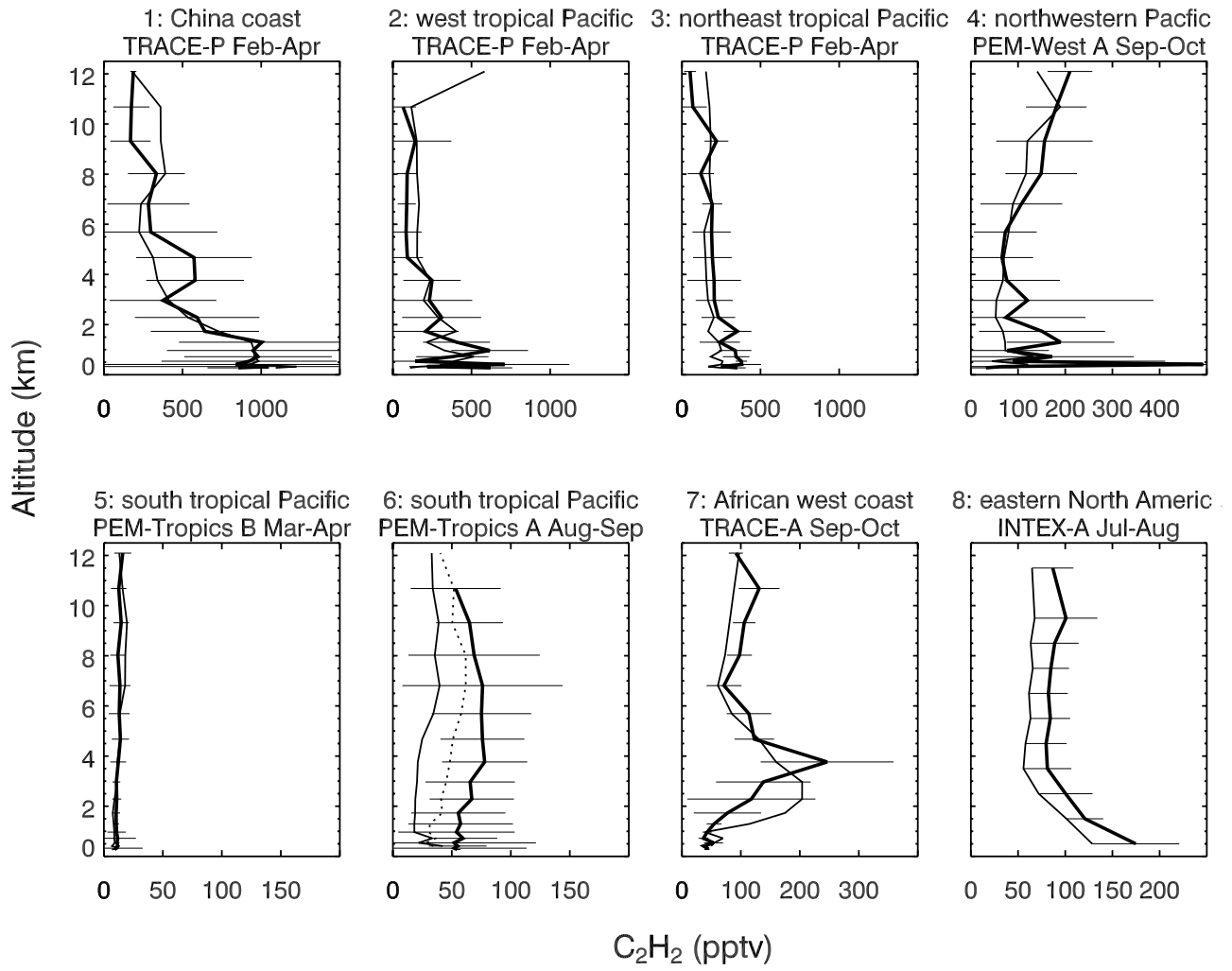

Figure 4. Simulated (thin lines) and observed (thick lines) vertical profiles of C_2H_2 concentrations from aircraft missions in different regions (Figure 1 and Table 2). The observations are mean values and standard deviations computed from 1-min average data. The model results are daily means along the flight tracks for year 2001 (TRACE-P mission year), except for INTEX-A which we compare to model results with 3-hour resolution for 2004. The dashed line in the region 6 panel shows PEM-Tropics A model simulation results for 1996 (when the mission was actually flown). Note differences in scales between panels, and the difference in vertical bins used for INTEX-A.

including a major contribution from biofuels. Over the west tropical Pacific in TRACE-P (region 2), the Asian influence has a relatively larger contribution from seasonal biomass burning in Southeast Asia [*Heald et al.*, 2003], and again this is well represented by the model. Background concentrations over the northeast tropical Pacific during TRACE-P (region 3) are also well simulated. PEM-West A over the same NW Pacific domain as TRACE-P but in August–September (region 4) observed a very different vertical profile, with weaker boundary layer outflow but strong convective enhancements in the upper troposphere [*Ehhalt et al.*, 1997]. The model reproduces this seasonal variation in the profile, as also found in a previous simulation of radionuclides in PEM-West A versus TRACE-P [*Liu et al.*, 2004]. It underestimates the boundary layer outflow in PEM-West A, but this likely reflects model errors in transport rather than in sources.

[20] Measurements over the South Pacific during PEM-Tropics B in February–March 1999 (region 5) sampled remarkably low concentrations, reflecting the seasonal minimum in the chemical lifetime and the lack of biomass burning influence [*Blake et al.*, 2001]. The average C_2H_2 concentration for that region is 9–16 pptv in the observations and 7–20 pptv in the model, with little vertical structure because of the strong convective environment. The same region during PEM-Tropics A in September–October 1996 (region 6) had a much higher median observed concentration of 65 pptv, reflecting biomass burning influence from Africa and South America transported over the South Pacific by strong subtropical westerlies [*Blake et al.*, 1999; *Board et al.*, 1999]. The model shows a low bias of 30 pptv compared to the observations that cannot be attributed to uncertainty in the C_2H_2 emission factor from biomass burning, since this factor varies only

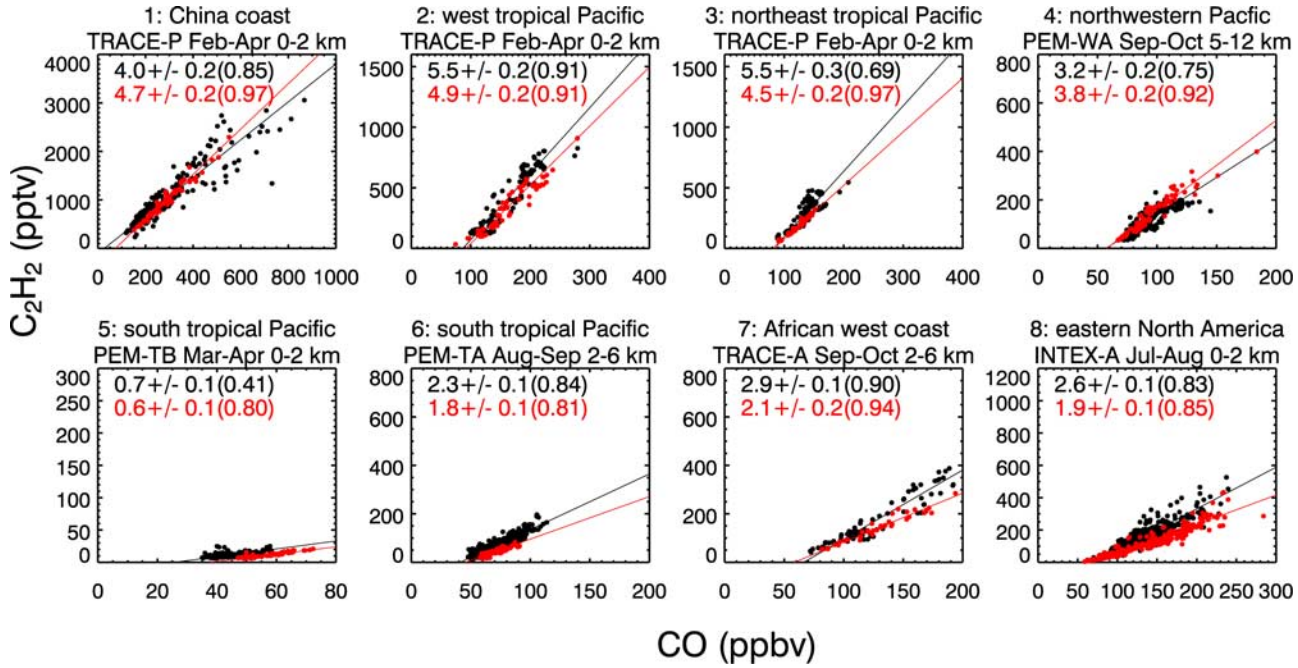

Figure 5. Simulated (red) versus observed (black) C_2H_2-CO relationships along the flight tracks for the aircraft missions of Figure 1. Reduced-major-axis regression lines are shown and the slopes (unit: 10^{-3} mol mol^{-1}) and coefficients of determination (r^2, in parentheses) are given inset. Standard deviations on the slopes are calculated by the bootstrap method. The model results used for comparison with PEM-Tropics A observations are from the simulation with 1996 meteorological fields. Note differences in scales between panels.

over a narrow range (Table 1), and the model gives a successful simulation of C_2H_2 concentrations in African biomass burning outflow during the TRACE-A aircraft mission in September–October 1992 (region 7 of Figure 4). A major factor for the bias appears to be interannual variability in transport, as the simulation using 1996 meteorology (dashed line) shows a reduction of 18 pptv (i.e., by 60%) in the bias. Meteorological conditions in 1996 were particularly conducive to transport of African biomass burning plumes over the South Pacific [*Fuelberg et al.*, 1999; *Staudt et al.*, 2002].

[21] Also shown in Figure 4 (region 8) are the simulated and observed vertical profiles of C_2H_2 over eastern North America during the INTEX-A mission (July August 2004). The observed C_2H_2 concentrations average 145 pptv in the boundary layer and 90 pptv in the free troposphere. The boundary layer enhancement in the model is due almost exclusively to US fossil fuel emissions; boreal forest fire influence is weak and vertically distributed, contributing on average 15 pptv to the vertical profile. The model is about 30 pptv too low throughout the profile, suggesting a 30% bias in background C_2H_2 at northern midlatitudes in summer. However, such a bias is not apparent in the surface and column data of Figures 2 and 3.

4. The C_2H_2-CO Relationship

[22] The aircraft missions in Figure 1 cover different regions of the world in different seasons. We examine here the C_2H_2-CO correlations and linear regressions in these different data sets and compare to results from the GEOS-Chem simulation. Our goal is to determine the information contained in the C_2H_2-CO relationships for testing model emissions, transport, and OH levels, and to better interpret these relationships as markers for air mass age. All linear regressions presented here use the reduced-major-axis method allowing for errors in both variables.

4.1. dC_2H_2/dCO Regression Slopes and Concentration Ratios

[23] Figure 5 shows the observed and simulated C_2H_2-CO enhancement ratios (subsequently called the dC_2H_2/dCO slopes) as determined by the slopes of the C_2H_2-CO reduced-major-axis regressions along the flight tracks for the aircraft missions of Figure 1. We focus on the regions of largest continental influence and variability as discussed in section 3; boundary layer (0–2 km) for TRACE-P, PEM-Tropics B, and INTEX-A; upper troposphere (>5 km) for PEM-West A; and free troposphere (2–6 km) for PEM-Tropics A and TRACE-A. All regions show strong correlations, both in the model and in the observations, with $r^2 >$ 0.4 in all cases and >0.8 in most. The slopes vary from 0.7 to 5.5 $\times$ 10^{-3} mol mol^{-1} depending on region, and the causes of these differences are discussed below.

[24] Observations in boundary layer outflow from China (TRACE-P) indicate a dC_2H_2/dCO slope of 4.0 $\times$ 10^{-3} mol mol^{-1}. The simulated dC_2H_2/dCO slope is 4.7 $\times$ 10^{-3} mol mol^{-1}, which is lower than the fuel (fossil + bio) emission ratio of 6.2 $\times$ 10^{-3} mol mol^{-1} used in the model for China. In the west tropical Pacific region of TRACE-P, the C_2H_2 and CO concentrations are reduced by about half relative to the boundary layer China outflow; however, the observed dC_2H_2/dCO slope (5.5 $\times$ 10^{-3} mol mol^{-1}) is actually higher. Similarly, we observe a high dC_2H_2/dCO slope of 5.5 $\times$ 10^{-3} mol mol^{-1} over the northeast tropical

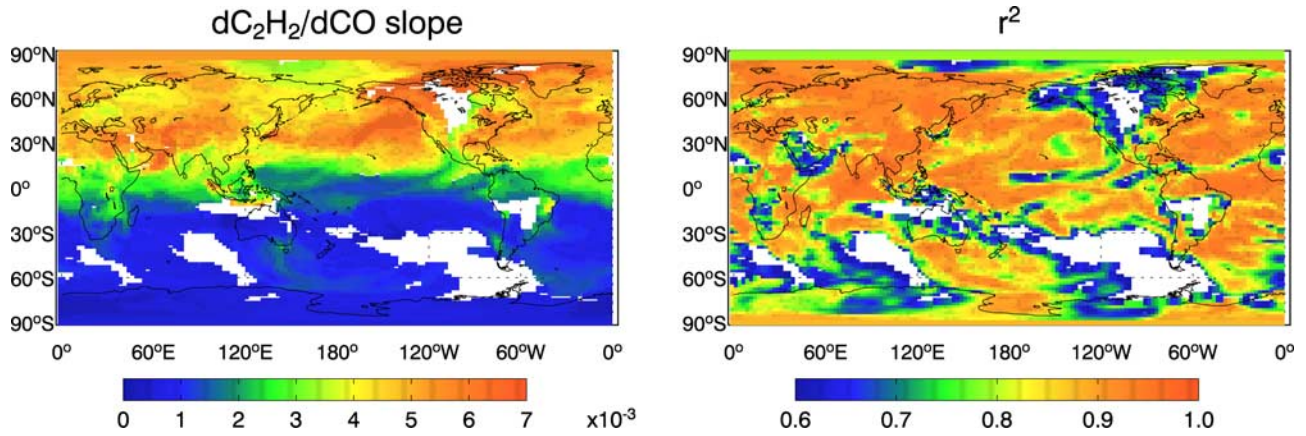

Figure 6. Simulated C_2H_2-CO correlations in the model for the boundary layer (<2 km) in March 2001. Left panel: slopes calculated by reduced-major-axis linear regression using the daily mean concentrations of C_2H_2 and CO in each model grid box. Right panel: coefficients of determination (r^2) for the linear regression. Areas with r^2<0.6 are left blank.

Pacific during TRACE-P (region 3), although this region was remote from continental influence. The model underestimates the slopes in regions 2 and 3, but it reproduces the qualitative result that the slopes do not decline during apparent aging. We find that the C_2H_2-CO correlations in regions 2 and 3 are driven in part by contrast between tropical air masses with low C_2H_2 and midlatitude air masses with high C_2H_2. A problem with interpreting C_2H_2-CO correlations to diagnose aging is the assumption that the background air anchoring the correlation is the same as the background air in which the polluted air dilutes. That assumption fails for regions 2 and 3.

[25] The slope observed over the NW Pacific above 5 km altitude during PEM-West A in August–September is 3.2×10^{-3} mol mol^{-1}, lower than in TRACE-P. The model (3.8×10^{-3} mol mol^{-1}) reproduces the relatively lower slope observed in PEM-West A than in TRACE-P, which can be attributed mainly to the influence of chemical aging. The simulated dC_2H_2/dCO slope in biomass burning outflow sampled over the African west coast during TRACE-A is 2.1×10^{-3} mol mol^{-1}, as compared to the observed slope of 2.9×10^{-3} mol mol^{-1}. It is lower than in Asian outflow because of the relatively low emission ratio from biomass burning (Table 1). A very low slope of 0.7×10^{-3} mol mol^{-1} is observed over the south tropical Pacific during PEM-Tropics B (region 5), consistent with the model (0.6×10^{-3} mol mol^{-1}) and reflecting the extensive aging.

[26] PEM-Tropics A observations over the South Pacific were influenced by biomass burning effluents transported from southern Africa and South America over typical timescales of 5–7 days [*Fuelberg et al.*, 1999; *Gregory et al.*, 1999; *Staudt et al.*, 2002]. The median C_2H_2 concentration observed in PEM-Tropics A is about 60% of that in TRACE-A outflow (70 pptv in region 6 versus 128 pptv in region 7). The observed dC_2H_2/dCO slope in PEM-Tropics A (2.3×10^{-3} mol mol^{-1}) is similar to that observed in TRACE-A (2.9×10^{-3} mol mol^{-1}). The simulated slopes in PEM-Tropics A and TRACE-A are also close to each other (1.8×10^{-3} mol mol^{-1} versus 2.1×10^{-3} mol mol^{-1}). Again, this appears to be due to difference between the background in which the biomass burning effluents are diluting versus the background anchoring the C_2H_2-CO correlation, as previously discussed by *Mauzerall et al.* [1998] for the interpretation of dO_3/dCO slopes in aged biomass burning plumes during TRACE-A. The background C_2H_2 and CO concentrations (as defined by the 10th percentiles of the data sets) are 30 pptv and 55 ppbv in PEM-Tropics A, versus 77 pptv and 85 ppbv in the African West Coast outflow of TRACE-A.

[27] The observed dC_2H_2/dCO slope in the North American boundary layer during INTEX-A is 2.6×10^{-3} mol mol^{-1}. The simulated slope is 1.9×10^{-3} mol mol^{-1}, reflecting model bias in simulating the C_2H_2 background (see section 3).

[28] Figure 6 shows the global distribution of the simulated dC_2H_2/dCO slopes in the boundary layer in March (corresponding to the timing of the TRACE-P and PEM-Tropics B aircraft campaigns). C_2H_2 and CO are strongly correlated ($r^2 > 0.6$) almost everywhere, with $r^2 > 0.85$ in most of the world. The dC_2H_2/dCO slope shows strong latitudinal gradient between the Northern and Southern Hemispheres. However, the Northern Hemisphere data do not show a trend of decreasing values from the source continents to the remote oceans. This demonstrates as discussed above that the dC_2H_2/dCO slope cannot be considered a robust tracer of air mass aging.

[29] Most previous analyses of the C_2H_2-CO pair as a tracer of air mass age have actually used the C_2H_2/CO concentration ratio, rather than the slope of the correlation, in part because it allows a diagnosis of age in individual observations rather than requiring ensembles of correlated observations. This turns out to be a much better indicator, albeit qualitative, of air mass aging. Figure 7 shows the global distributions of the simulated and observed C_2H_2/CO concentration ratios in the boundary layer in March. The observed C_2H_2/CO molar ratio varies from $4–6 \times 10^{-3}$ in Asian outflow to $1–3 \times 10^{-3}$ over the remote North Pacific and less than 1×10^{-3} in the southern hemisphere. The C_2H_2/CO ratio shows a gradual zonal decrease from western to eastern Pacific both in the observations and the model, which can be understood simply in terms of aging but is not seen in the dC_2H_2/dCO slopes of Figure 6.

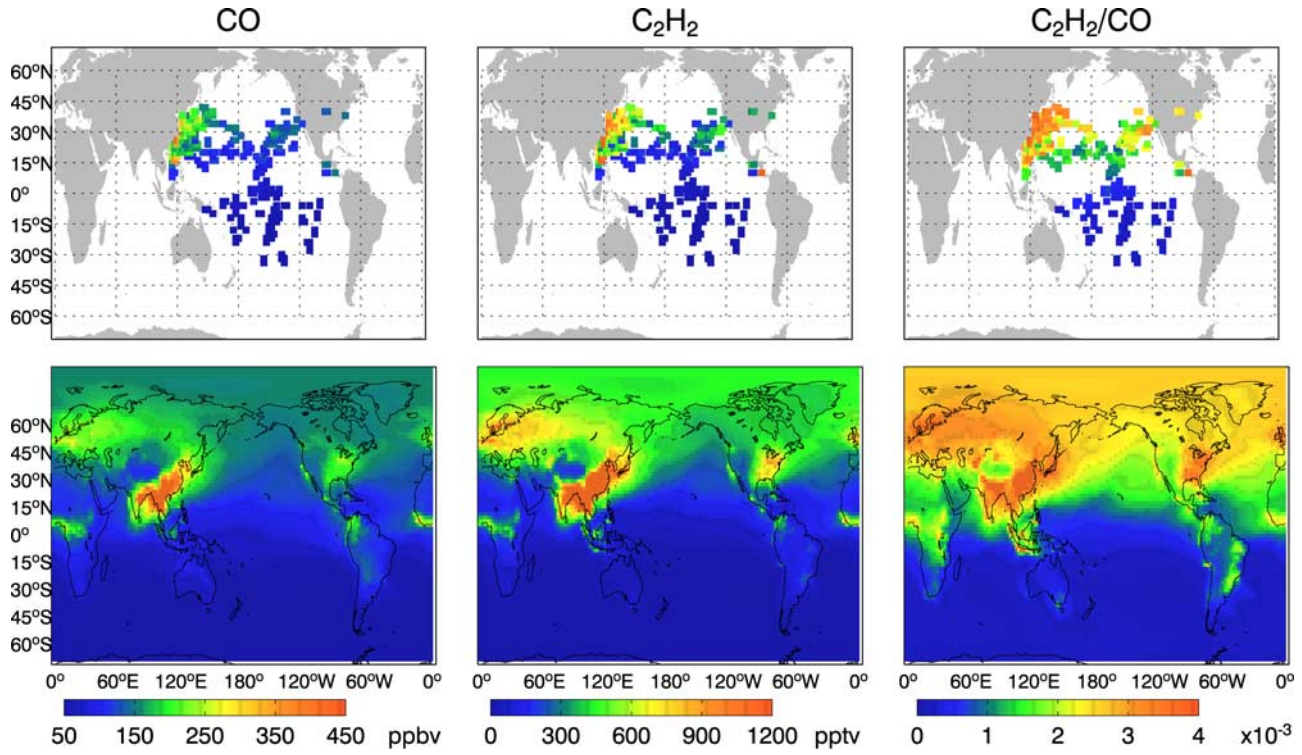

Figure 7. Observed (top) versus simulated (bottom) CO and C_2H_2 concentrations, and C_2H_2/CO molar concentration ratios, in the boundary layer (0–2 km) in March. The observations are from the TRACE-P and PEM-Tropics B aircraft missions. The model results are monthly means for 2001. Color scales saturate at the maximum values indicated on the color bars.

4.2. dlog[C_2H_2]/dlog[CO] Regression Slopes

[30] Examination of the relationship between the logarithms of concentrations for two species with common sources offers insight into the relative contributions of dilution and chemical aging in a manner that is independent of the emission ratio [*McKeen and Liu*, 1993, *McKeen et al.*, 1996; *Ehhalt et al.*, 1998]. Consider two such species i and j, and let β be the slope of the log-log concentration relationship: β = dln (M_j)/dln (M_i). *McKeen et al.* [1996] proposed a linear mixing model to interpret β based on the Lagrangian mass balance equation:

$$\frac{dM_i}{dt} = -L_i \cdot M_i - K_{dil}\left(M_i - M_i^{bg}\right) \quad (1)$$

where M_i is the concentration of species i, L_i is its first-order loss frequency (i.e., k_i[OH], where k_i is the reaction rate constant for reaction with OH), K_{dil} is a dilution rate constant (s^{-1}), and M_i^{bg} is the background concentration. Assumption of a single point source together with constant values for K_{dil}, L_i, and M_i^{bg} yields simple analytical relationships in limiting cases. If chemical loss is fast relative to dilution (L_i and L_j both $\gg K_{dil}$), then $\beta \approx L_i / L_j = \tau_j / \tau_i$, where τ_i is the chemical lifetime of species i. If dilution is significant relative to chemical loss but the background concentrations are negligible, then a linear relationship in log space can still be expected with a weaker slope $\beta \approx (K_{dil} + L_j) / (K_{dil} + L_i)$; in the limiting case where dilution dominates over chemical loss, β tends toward unity.

[31] In the case of C_2H_2 and CO, the chemical lifetimes are relatively long and the background concentrations are nonnegligible, so no simple analytical approximation for β can be made from the *McKeen et al.* [1996] model. In an application to data from the PEM-West A mission over the northwestern Pacific with independent estimate of K_{dil}, *McKeen et al.* [1996] and *Smyth et al.* [1996] concluded that the C_2H_2/CO log-log concentration relationship in Asian outflow would be determined mainly by dilution rather than by chemistry. As we will see below from OH sensitivity studies in GEOS-Chem, this is indeed the case for fresh outflow but not for more aged air.

[32] *Ehhalt et al.* [1998] presented a more general framework for interpretation of log-log concentration relationships. They showed that a one-dimensional (vertical) diffusive transport model yields a different form for β than the linear mixing model of *McKeen et al.* [1996]. The continuity equation for species i in that model is:

$$\frac{\partial M_i}{\partial t} = -L_i \cdot M_i + D \cdot \frac{\partial^2 M_i}{\partial z^2} \quad (2)$$

[33] Assuming a constant turbulent diffusion coefficient D and constant loss frequency L_i, the steady state solution for the vertical profile $M_i(z)$ subject to the boundary conditions $M_i(0) = M_{i,0}$ and $M_i(\infty) = 0$ is:

$$M_i(z) = M_{i,0} e^{-z/\sqrt{D/L_i}} \quad (3)$$

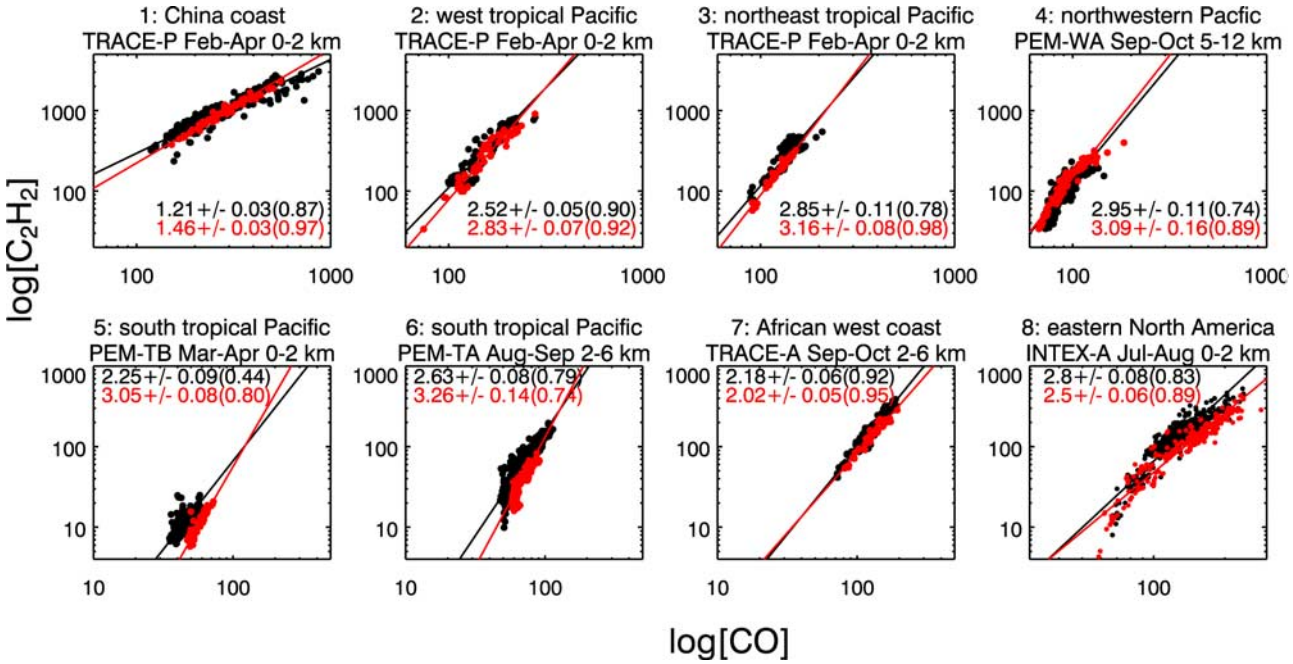

Figure 8. Same as Figure 5 but for log[C_2H_2]-log[CO].

[34] This model yields a linear log-log relationship between species i and j with slope $\beta = \sqrt{\tau_i/\tau_j}$. *Ehhalt et al.* [1998] presented illustrative simulations with a three-dimensional CTM indicating that β varies with the relative importance of dilution versus photochemical loss. For $\beta = 1$, the decline is only due to dilution acting on both species at the same rate, in the same way as the *McKeen et al.* [1996] model. $\beta = \sqrt{\tau_i/\tau_j}$ indicates that dilution and chemical decay act at comparable rates. $\beta > \sqrt{\tau_i/\tau_j}$ (where $\tau_i > \tau_j$) indicates that chemical decay dominates over dilution. For the C_2H_2-CO pair, the lifetime ratio τ_{CO}/τ_{C2H2} remains in a narrow range 3–3.5 ($\sqrt{\tau_{CO}/\tau_{C2H2}}$ is in the range 1.7–1.9) throughout the troposphere. Such a narrow range makes C_2H_2-CO an attractive pair for testing the interpretation of β in terms of the *Ehhalt et al.* [1998] model.

[35] Figure 8 shows the simulated versus observed dlog[C_2H_2]-dlog[CO] relationships along the flight tracks for the previously discussed aircraft data sets. The β = dlog[C_2H_2]/dlog[CO] slopes are higher in remote marine regions than in continental outflow, both in the model and in the observations. The lowest value (1.2) is in fresh boundary layer China outflow (region 1), reflecting dilution of continental emissions with little chemical loss. All other values are higher than 1.8, suggesting that chemistry dominates over dilution in determining the aging. The model generally reproduces the geographical variation of the log-log slopes but is too high over the South Pacific, by 35% in regions 5 and 6.

[36] Remarkably, even though one would expect Eulerian models such as GEOS-Chem to have excessive diffusion due to the advection algorithm, we find no systematic low bias in the log-log slopes that would indicate such numerical diffusion. *Wild and Prather* [2006] suggest that the effect of numerical diffusion may be artificially compensated by model smoothing of horizontal winds.

[37] To test the actual relative importance of chemical aging versus dilution in GEOS-Chem, we conducted model simulations with OH increased or decreased uniformly by 50% and examined the sensitivity of the dlog[C_2H_2]/dlog[CO] slope. Results are shown in Figure 9. The simulated slopes show least sensitivity to OH in the Asian and African fresh outflow (regions 1 and 7), highest sensitivity over the South Pacific (region 5 and 6) where the model slopes are highest, and moderate sensitivity over the northwestern Pacific (region 4) and eastern North America (region 8) in summer. Although the *Ehhalt et al.* [1998] model would diagnose the β value for region 7 as indicative of preferential chemical aging, we find that it is in fact largely driven by dilution, as would be expected for fresh outflow.

[38] The sensitivity of β to OH concentrations over the South Pacific, combined with the model overestimate of β, suggests a model overestimate of OH in that region. Matching the observed β would require decreasing model OH by more than a factor of 2 (Figure 9). We pointed out previously that the model can not be in such error in its simulation of the global mean OH concentration (as constrained by methylchloroform concentrations) or the OH concentration at northern midlatitudes (as constrained by the relative seasonal variation of C_2H_2). Further investigation is needed of a possible error in the OH simulation in the southern tropics.

5. Conclusions

[39] Acetylene and carbon monoxide are strongly correlated in atmospheric observations worldwide, reflecting commonality of sources (combustion) and sink (oxidation by OH). They have different lifetimes, about two weeks for C_2H_2 and two months for CO. The evolution of the C_2H_2-CO relationship downwind of continental source regions

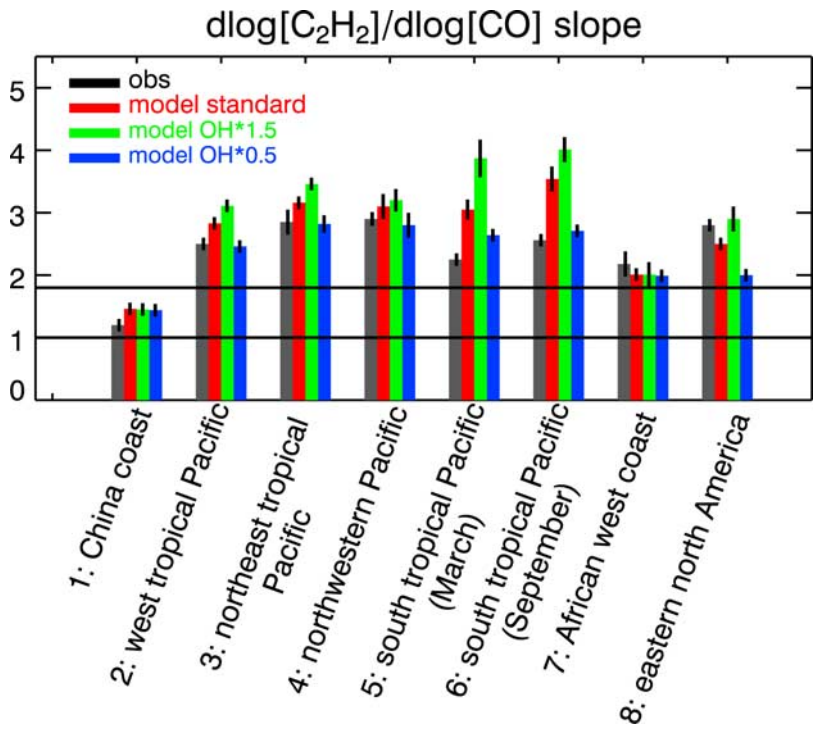

Figure 9. dlog[C_2H_2]/dlog[CO] slopes (β) for the aircraft regions of Figure 1. Observations (black) are compared to values from the standard model (red) and sensitivity simulations with OH uniformly increased by 50% (green) or decreased by 50% (blue). The error bars are standard deviations of the slopes calculated by the bootstrap method. Also shown are horizontal lines of 1 (aging controlled by dilution) and 1.8 (mean square root of the ratio of lifetimes, implying comparable contributions of dilution and chemistry to aging in the *Ehhalt et al.* [1998] model).

and extending to the remote troposphere offers information on dilution and chemical aging of polluted air masses. We used here observations from a number of aircraft campaigns in different regions of the world to diagnose and interpret the relationships between C_2H_2 and CO concentrations in terms of concentration ratios, linear regression slopes, and log-log linear regression slopes. We compared the results to idealized models for dilution and chemical aging [*McKeen and Liu*, 1993, *McKeen et al.*, 1996; *Ehhalt et al.*, 1998] as well as to results from the GEOS-Chem chemical transport model (CTM). Our goal was to provide a quantitative framework for interpreting C_2H_2-CO relationships in atmospheric observations, and to use these relationships as a test of air mass aging in GEOS-Chem.

[40] The first step in our analysis was to construct a global budget of atmospheric C_2H_2 in GEOS-Chem and evaluate it with observations. The global mean tropospheric lifetime of C_2H_2 in GEOS-Chem is 12 days against oxidation by OH, its only significant sink. Our best estimate of C_2H_2 sources includes 1.7 Tg yr^{-1} from fossil fuels, 3.3 Tg yr^{-1} from biofuels, and 1.6 Tg yr^{-1} from biomass burning. The resulting model can simulate the ensemble of global C_2H_2 observations without systematic bias, and captures most seasonal and regional features. The large biofuel source is consistent with aircraft observations in Asian outflow. Our total C_2H_2 source strength of 6.6 Tg yr^{-1} is higher than the 3.1 Tg yr^{-1} previously estimated by *Gupta et al.* [1998] using C_2H_2 concentration data at remote sites as constraints in a two-dimensional zonally averaged model. Reliance on remote data to constrain sources in a two-dimensional model would be expected to cause a low bias.

[41] The global distribution of the C_2H_2/CO concentration ratio shows a decrease from continental source regions to the remote atmosphere, both in the model and observations, reflecting the utility of that ratio as a qualitative tracer of air mass age extending to the remote troposphere. However, we find that the dC_2H_2/dCO slopes derived from linear regressions of concentrations cannot be used for this purpose, as they show no systematic decrease between fresh continental outflow and remote oceanic air either in the model or in the observations. This result reflects variability in the background air driving the correlation. If the background air in which the continental outflow is diluting is different from that anchoring the correlation in the remote region, then the C_2H_2-CO regression will reflect the sampling of these distinct air masses rather than dilution or oxidation processes.

[42] The slope of the C_2H_2-CO relationship in log space (slope β of the linear regression in a log-log plot of concentrations) allows an examination of the relative contributions of dilution and chemical aging. *McKeen et al.* [1996] and *Ehhalt et al.* [1998] presented theoretical models for the interpretation of β. We find that a simple linear mixing model with constant dilution and background, as proposed by *McKeen et al.* [1996] is adequate in fresh continental outflow where aging is mainly from dilution. It

is inadequate for more remote conditions. *Ehhalt et al.* [1998] offer a more general model framework for interpreting the observed log-log relationships in remote air. In that model, a β value equal to the square root of the ratios of chemical lifetimes (1.8 for the C_2H_2-CO pair) indicates comparable contributions from dilution and chemical aging; lower values of β indicate a dominance from dilution, and higher values indicate a dominance from chemistry. This model suggests that aging of air in remote regions as diagnosed by the log[C_2H_2]-log[CO] relationship is driven by chemical loss more than by dilution.

[43] The GEOS-Chem CTM generally reproduces the values of β observed for the different regions, in particular the gradient between continental air and remote oceanic air. Sensitivity simulations with modified OH concentrations show that β is insensitive to OH in continental outflow (where aging is controlled by dilution) but sensitive to OH in remote air (where aging is controlled by chemistry). Model values of β are biased high over the South Pacific. A sensitivity simulation with OH concentrations reduced by 50% significantly reduces the magnitude of the bias, suggesting that model OH concentrations in that region may be overestimated.

[44] **Acknowledgments.** This work was funded by the Atmospheric Chemistry Program of the US National Science Foundation. We would like to thank Jennifer Logan, Stuart McKeen, and Bill Munger for helpful discussions. We thank Justus Notholt for providing averaging kernel information for column observations of C_2H_2. We thank Hongyu Liu for helping to set up the GEOS-Chem simulation for the year 1996. We also thank Rynda Hudman and Inna Megretskaia for help with processing the C_2H_2 data from aircraft missions.

References

Andreae, M. O., and P. Merlet (2001), Emission of trace gases and aerosols from biomass burning, *Glob. Biogeochem. Cycles*, *15*(4), 955–966.

Atkinson, R. (2000), Atmospheric chemistry of VOCs and NOx, *Atmos. Environ.*, *34*, 2063–2101.

Barletta, B., S. Meinardi, F. S. Rowland, C. Y. Chan, X. M. Wang, S. C. Zou, L. Y. Chan, and D. R. Blake (2005), Volatile organic compounds in 43 Chinese cities, *Atmos. Environ.*, *39*(32), 5979–5990.

Bertschi, I. T., R. J. Yokelson, D. E. Ward, T. J. Christian, and W. M. Hao (2003), Trace gas emissions from the production and use of domestic biofuels in Zambia measured by open-path Fourier transform infrared spectroscopy, *J. Geophys. Res.*, *108*(D13), 8469, doi:10.1029/2002JD002158.

Bey, I., D. J. Jacob, R. M. Yantosca, J. A. Logan, B. Field, A. M. Fiore, Q. Li, H. Liu, L. J. Mickley, and M. Schultz (2001), Global modeling of tropospheric chemistry with assimilated meteorology: Model description and evaluation, *J. Geophys. Res.*, *106*, 23,073–23,096.

Blake, D. R., D. F. Hurst, T. W. Smith, W. J. Whipple, T. Y. Chen, N. J. Blake, and F. S. Rowland (1992), Summertime measurements of selected nonmethane hydrocarbons in the Arctic and sub-Arctic during the 1998 Arctic Boundary-layer Expedition (ABLE-3A), *J. Geophys. Res.*, *97*(D15), 16,559–16,588.

Blake, N. J., S. A. Penkett, K. C. Clemitshaw, P. Anwyl, P. Lightman, A. R. W. Marsh, and G. Butcher (1993), Estimates of atmospheric hydroxyl radical concentrations from the observed decay of many reactive hydrocarbons in well-defined urban plumes, *J. Geophys. Res.*, *98*(D2), 2851–2864.

Blake, D. R., T. Y. Chen, T. Y. Smith, C. J. L. Wang, O. W. Wingenter, N. J. Blake, F. S. Rowland, and E.W. Mayer (1996), Three-dimensional distribution of nonmenthane hydrocarbons and halocarbons over the northwestern Pacific during the 1991 Pacific Exploratory Mission (PEM-West A), *J. Geophys. Res.*, *101*(D1), 1763–1778.

Blake, N. J., et al. (1999), Influence of southern hemispheric biomass burning on midtropospheric distributions of nonmethane hydrocarbons and selected halocarbons over the remote South Pacific, *J. Geophys. Res.*, *104*(D13), 16,213–16,232.

Blake, N. J., et al. (2001), Large-scale latitudinal and vertical distributions of NMHCs and selected halocarbons in the troposphere over the Pacific Ocean during the March–April 1999 Pacific Exploratory Mission (PEM-Tropics B), *J. Geophys. Res.*, *106*(D23), 32,627.

Blake, N. J., D. R. Blake, B. C. Sive, A. S. Katzenstein, S. Meinardi, O. W. Wingenter, E. L. Atlas, F. Flocke, B. A. Ridley, and F. S. Rowland (2003), The seasonal evolution of NMHCs and light alkyl nitrates at middle to high northern latitudes during TOPSE, *J. Geophys. Res.*, *108*(D4), 8359, doi:10.1029/2001JD001467.

Board, A. S., H. E. Fuelberg, G. L. Gregory, B. G. Heikes, M. G. Schultz, D. R. Blake, J. E. Dibb, S. T. Sandholm, and R. W. Talbot (1999), Chemical characteristics of air from differing source regions during the Pacific Exploratory Mission-Tropics A (PEM-Tropics A), *J. Geophys. Res.*, *104*(D13), 16,181–16,196.

Carmichael, G. R., et al. (2003), Evaluating regional emission estimates using the TRACE-P observations, *J. Geophys. Res.*, *108*(D21), 8810, doi:10.1029/2002JD003116.

de Gouw, J. A., et al. (2005), Budget of organic carbon in a polluted atmosphere: Results from the New England Air Quality Study in 2002, *J. Geophys. Res.*, *110*, D16305, doi:10.1029/2004JD005623.

DeMore, W. B. et al. (1997) Chemical kinetics and photochemical data for use in stratospheric modeling, JPL Publ. 97-4.

Duncan, B. N., and I. Bey (2004), A modeling study of export pathways of pollution from Europe: Seasonal and Interannual variations (1987–1997), *J. Geophys. Res.*, *109*, D08301, doi:10.1029/2003JD004079.

Duncan, B. N., R. V. Martin, A. C. Staudt, R. Yevich, and J. A. Logan (2003), Interannual and seasonal variability of biomass burning emissions constrained by satellite observations, *J. Geophys. Res.*, *108*(D2), 4040, doi:10.1029/2002JD002378.

Ehhalt, D. H., F. Rohrer, A. B. Kraus, M. J. Prather, D. R. Blake, and F. S. Rowland (1997), On the significance of regional trace gas distributions as derived from aircraft campaigns in PEM-West A and B, *J. Geophys. Res.*, *102*(D23), 28,333–28,351.

Ehhalt, D. H., F. Rohrer, A. Wahner, M. J. Prather, and D. R. Blake (1998), On the use of hydrocarbons for the determination of tropospheric OH concentrations, *J. Geophys. Res.*, *103*(D15), 18,981–18,997.

Fiore, A. M., D. J. Jacob, H. Liu, R. M. Yantosca, T. D. Fairlie, and Q. Li (2003), Variability in surface ozone background over the United States: Implications for air quality policy, *J. Geophys. Res.*, *108*, (D24), 4787, doi:10.1029/2003JD003855.

Fishman, J., J. M. Hoell, R. D. Bendura, R. J. McNeil, and V. W. J. H. Kirchhoff (1996), NASA GTE TRACE A experiment (September October 1992): Overview, *J. Geophys. Res.*, *101*(D19), 23,865–23,879.

Fortin, T. J., B. J. Howard, D. D. Parrish, P. D. Goldan, W. C. Kuster, E. L. Atlas, and R. A. Harley (2005), Temporal changes in US benzene emissions inferred from atmospheric measurements, *Environ. Sci. Technol.*, *39*(6), 1403–1408.

Fuelberg, H. E., R. E. Newell, S. P. Longmore, Y. Zhu, D. J. Westberg, E. V. Browell, D. R. Blake, G. L. Gregory, and G. W. Sachse (1999), A meteorological overview of the Pacific Exploratory Mission (PEM) Tropics period, *J. Geophys. Res.*, *104*(D5), 5585–5622.

Gautrois, M., T. Brauers, R. Koppmann, F. Rohrer, O. Stein, and J. Rudolph (2003), Seasonal variability and trends of volatile organic compounds in the lower polar troposphere, *J. Geophys. Res.*, *108*(D13), 4393, doi:10.1029/2002JD002765.

Goldstein, A. H., S. C. Wofsy, and C. M. Spivakovsky (1995), Seasonal variations of nonmethane hydrocarbons in rural New England: constraints on OH concentrations in northern midlatitudes, *J. Geophys. Res.*, *100*(D10), 21,023–21,033.

Gregory, G. L., J. T. Merrill, M. C. Shipham, D. R. Blake, G. W. Sachse, and H. B. Singh (1997), Chemical characteristics of tropospheric air over the Pacific Ocean as measured during PEM-West B: Relationship to Asian outflow and trajectory history, *J. Geophys. Res.*, *102*, 28,275–28,285.

Gregory, G. L., et al. (1999), Chemical characteristics of Pacific tropospheric air in the region of the Intertropical Convergence Zone and South Pacific Convergence Zone, *J. Geophys. Res.*, *104*(D5), 5677–5696.

Grosjean, E., R. A. Rasmussen, and D. Grosjean (1998), Ambient levels of gas phase pollutants in Porto Alegre, Brazil, *Atmos. Environ.*, *32*(22), 3371–3379.

Gupta, M. L., R. J. Cicerone, D. R. Blake, F. S. Rowland, and I. S. A. Isaksen (1998), Global atmospheric distributions and source strengths of light hydrocarbons and tetrachloroethene, *J. Geophy. Res.*, *103*, 28,219–28,235.

Hao, W. M., D. E. Ward, G. Olbu, and S. P. Baker (1996), Emissions of CO_2, CO, and hydrocarbons from fires in diverse African savanna ecosystems, *J. Geophys. Res.*, *101*(D19), 23,577–23,584.

Harley, R. A., S. A. McKeen, J. Pearson, M. O. Rodgers, and W. A. Lonneman (2001), Analysis of motor vehicle emissions during the Nashville/Middle Tennessee Ozone Study, *J. Geophys. Res.*, *106*(D4), 3559–3567.

Heald, C. L., D. J. Jacob, P. I. Palmer, M. J. Evans, G. W. Sachse, H. B. Singh, and D. R. Blake (2003), Biomass burning emission inventory with

daily resolution: Application to aircraft observations of Asian outflow, *J. Geophys. Res.*, *108*(D21), 8811, doi:10.1029/2002JD003082.

Heald, C. L., D. J. Jacob, D. B. A. Jones, P. I. Palmer, J. A. Logan, D. G. Streets, G. W. Sachse, J. C. Gille, R. N. Hoffman, and T. Nehrkorn (2004), Comparative inverse analysis of satellite (MOPITT) and aircraft (TRACE-P) observations to estimate Asian sources of carbon monoxide, *J. Geophys. Res.*, *109*, D23306, doi:10.1029/2004JD005185.

Hegg, D. A., L. F. Radke, P. V. Hobbs, R. A. Rasmussen, and P. J. Riggan (1990), Emissions of some tracer gases from biomass fires, *J. Geophys. Res.*, *95*(D5), 5669–5675.

Hoell, J. M., D. Davis, S. C. Liu, R. Newell, M. Shipham, H. Akimoto, R. J. McNeal, R. J. Bendura, and J. W. Drewry (1996), Pacific exploratory Mission-West A (PEM-West A): September–October 1991, *J. Geophys. Res.*, *101*(D1), 1641–1653.

Hoell, J. M., D. D. Davis, D. J. Jacob, M. O. Rodgers, R. E. Newell, H. E. Fuelberg, R. J. McNeal, J. L. Raper, and R. J. Bendura (1999), Pacific Exploratory Mission in the tropical Pacific: PEM-Tropics A, August–September 1996, *J. Geophys. Res.*, *104*(D5), 5567–5583.

Hudman, R. C., et al. (2007), Surface and lightning sources of nitrogen oxides over the United States: magnitudes, chemical evolution, and outflow, *J. Geophys. Res.*, *112*, D12505, doi:10.1029/2006JD007912.

Jacob, D. J., J. H. Crawford, M. M. Kleb, V. S. Connors, R. J. Bendura, J. L. Raper, G. W. Sachse, J. C. Gille, L. Emmons, and C. L. Heald (2003), The Transport and Chemical Evolution over the Pacific (TRACE-P) aircraft mission: design, execution, and first results, *J. Geophys. Res.*, *108*(D20), 9000, doi:10.1029/2002JD003276.

Jaeglé, L., D. A. Jaffe, H. U. Price, P. Weiss-Penzias, P. I. Palmer, M. J. Evans, D. J. Jacob, and I. Bey (2003), Sources and budgets for CO and O3 in the Northeastern Pacific during the spring of 2001: Results from the PHOBEA-II Experiment, *J. Geophys. Res.*, *108*(D20), 8802, doi:10.1029/2002JD003121.

Kanakidou, M., B. Bonsang, J. C. Le Roulley, G. Lambert, D. Martin, and G. Sennequier (1988), Marine source of atmospheric acetylene, *Nature*, *333*(6168), 51–52.

Laurila, T., and H. Hakola (1996), Seasonal cycle of C_2–C_5 hydrocarbons over the Baltic Sea and Northern Finland, *Atmos. Environ.*, *30*(10–11), 1597–1607.

Liang, Q., L. Jaegle, D. A. Jaffe, P. Weiss-Penzias, A. Heckman, and J. A. Snow (2004), Long-range transport of Asian pollution to the northeast Pacific: Seasonal variations and transport pathways of carbon monoxide, *J. Geophys. Res.*, *109*(D23), D23S07, doi:10.1029/2003JD004402.

Lin, S. J., and R. B. Rood (1996), Multidimensional flux-form semi-Lagrangian transport schemes, *Mon. Weather Rev.*, *124*(9), 2046–2070.

Liu, H., D. J. Jacob, I. Bey, R. M. Yantosca, B. N. Duncan, and G. W. Sachse (2003), Transport pathways for Asian combustion outflow over the Pacific: Interannual and seasonal variations, *J. Geophys. Res.*, *108*(D20), 8786, doi:10.1029/2002JD003102.

Liu, H., D. J. Jacob, J. E. Dibb, A. M. Fiore, and R. M. Yantosca (2004), Constraints on the sources of tropospheric ozone from ^{210}Pb–^{7}Be–O_3 correlations, *J. Geophys. Res.*, *109*, D07306, doi:10.1029/2003JD003988.

Mahieu, E., R. Zander, L. Delbouille, P. Demoulin, G. Roland, and C. Servais (1997), Observed trends in total vertical column abundances of atmospheric gases from IR solar spectra recorded at the Jungfraujoch, *J. Atmos. Chem.*, *28*(1–3), 227–243.

Mauzerall, D. L., J. A. Logan, D. J. Jacob, B. E. Anderson, D. R. Blake, J. D. Bradshaw, B. Heikes, G. W. Sachse, H. Singh, and B. Talbot (1998), Photochemistry in biomass burning plumes and implications for tropospheric ozone over the tropical South Atlantic, *J. Geophys. Res.*, *103*(D7), 8401–8423.

McKeen, S. A., and S. C. Liu (1993), Hydrocarbon ratios and photochemical history of air masses, *Geophys. Res. Lett.*, *20*(21), 2363–2366.

McKeen, S. A., S. C. Liu, E. Y. Hsie, X. Lin, J. D. Bradshaw, S. Smyth, G. L. Gregory, and D. R. Blake (1996), Hydrocarbon ratios during PEM-WEST A: A model perspective, *J. Geophys. Res.*, *101*(D1), 2087–2109.

Moorthi, S., and M. J. Suarez (1992), Relaxed Arakawa-Schubert: A parameterization of moist convection for general circulation models, *Mon. Weather Rev.*, *120*, 978–1002.

Notholt, J., G. Toon, F. Stordal, S. Solberg, N. Schmidbauer, E. Becker, A. Meier, and B. Sen (1997), Seasonal variations of atmospheric trace gases in the high Arctic at 79 degrees N, *J. Geophys. Res.*, *102*(11D), 12,855–12,861.

Olivier, J. G. J., et al. (1996) Description of EDGAR Version 2.0, RIVM/TNO report 771060002, RIVM, Bilthoven, December.

Palmer, P. I., D. J. Jacob, D. B. Jones, C. L. Heald, R. M. Yantosca, J. A. Logan, G. W. Sachse, and D. G. Streets (2003), Inverting for emissions of carbon monoxide from Asia using aircraft observations over the western Pacific, *J. Geophys. Res.*, *108*(D21), 8828, doi:10.1029/2003JD003397.

Parrish, D. D. (2006), Critical evaluation of US on-road vehicle emission inventories, *Atmos. Environ.*, *40*, 2288–2300.

Parrish, D. D., C. J. Hahn, E. J. Williams, R. B. Norton, F. C. Fehsenfeld, H. B. Singh, J. D. Shetter, B. W. Gandrud, and B. A. Ridley (1992), Indications of photochemical histories of Pacific air masses from measurements of atmospheric trace species at Point Arena, California, *J. Geophys. Res.*, *97*, 15,883–15,901.

Parrish, D. D., Y. Kondo, O. R. Cooper, C. A. Brock, D. A. Jaffe, M. Trainer, T. Ogawa, G. Hubler, and F. C. Fehsenfeld (2004), Intercontinental Transport and Chemical Transformation 2002 (ITCT 2K2) and Pacific Exploration of Asian Continental Emission (PEACE) experiments: An overview of the 2002 winter and spring intensives, *J. Geophys. Res.*, *109*(D23), 111, D23S01, doi:10.1029/2004JD004980.

Penkett, S. A., N. J. Blake, P. Lightman, A. R. W. Marsh, P. Anwyl, and G. Butcher (1993), The seasonal variation of nonmethane hydrocarbons in the free troposphere over the North Atlantic Ocean: Possible evidence for extensive reaction of hydrocarbons with the nitrate radical, *J. Geophys. Res.*, *98*(D2), 2865–2885.

Pierson, W. R., A. W. Gertler, N. F. Robinson, J. C. Sagebiel, B. Zielinska, G. A. Bishop, D. H. Stedman, R. B. Zweidinger, and W. D. Ray (1996), Real-world automotive emissions—Summary of studies in the Fort McHenry and Tuscarora Mountain Tunnels, *Atmos. Environ.*, *30*(12), 2233–2256.

Plass-Dulmer, C., R. Koppmann, M. Ratte, and J. Rudolph (1995), Light nonmethane hydrocarbons in seawater, *Glob. Biogeochem. Cycles*, *9*, 79–100.

Prinn, R. G., et al. (2001), Evidence for substantial variations of atmospheric hydroxyl radical in the past two decades, *Science*, *292*, 1882–1887.

Raper, J. L., M. M. Kleb, D. J. Jacob, D. D. Davis, R. E. Newell, H. E. Fuelberg, R. J. Bendura, J. M. Hoell, and R. J. McNeal (2001), Pacific Exploratory Mission in the tropical Pacific: PEM-Tropics B, March-April 1999, *J. Geophys. Res.*, *106*(D23), 32,401–32,425.

Rinsland, C. P., et al. (1999), Infrared solar spectroscopic measurements of free tropospheric CO, C_2H_6, and HCN above Mauna Loa, Hawaii: Seasonal variations and evidence for enhanced emissions from the Southeast Asian tropical fires of 1997–1998, *J. Geophys. Res.*, *104*, 18,667–18,680.

Russo, R. S., et al. (2003), Chemical composition of Asian continental outflow over the western Pacific: Results from Transport and Chemical Evolution over the Pacific (TRACE-P), *J. Geophys. Res.*, *108*(D20), 8804, doi:10.1029/2002JD003184.

Sigsby, J. E., S. T. Jr., W. Ray, J. M. Lang, and J. W. Duncan (1987), Volatile organic compound emissions from 46 in-use passenger cars, *Environ. Sci. Technol.*, *21*, 466–475.

Singh, H. B., W. H. Brune, J. H. Crawford, and D. J. Jacob (2006), Overview of the summer 2004 Intercontinental Chemical Transport Experiment-North America (INTEX-A), *J. Geophys. Res.*, *111*, D24501, doi:10.1029/2006JD007905.

Smyth, S., et al. (1996), Comparison of free tropospheric western Pacific air mass classification schemes for the PEM-West A experiment, *J. Geophys. Res.*, *101*(D1), 1743–1762.

Solberg, S., C. Dye, N. Schmidbauer, A. Herzog, and G. Gehrig (1996), Carbonyls and nonmethane hydrocarbons at rural European sites from the Mediterranean to the Arctic, *J. Atmos. Chem.*, *25*(1), 33–66.

Staudt, A. C., D. J. Jacob, J. A. Logan, D. Bachiochi, T. N. Krishnamurti, and N. Poisson (2002), Global chemical model analysis of biomass burning and lightning influences over the South Pacific in austral spring, *J. Geophys. Res.*, *107*(D14), 4200, doi:10.1029/2000JD000296.

Streets, D. G., et al. (2003), An inventory of gaseous and primary aerosol emissions in Asia in the year 2000, *J. Geophys. Res.*, *108*(D21), 8809, doi:10.1029/2002JD003093.

Swanson, A. L., N. J. Blake, E. Atlas, F. Flocke, D. R. Blake, and F. S. Rowland (2003), Seasonal variations of C_2–C_4 nonmethane hydrocarbons and C_1–C_4 alkyl nitrates at the Summit research station in Greenland, *J. Geophys. Res.*, *108*(D2), 4065, doi:10.1029/2001JD001445.

Turquety, S., et al. (2007), Inventory of boreal fire emissions for North America in 004: The importance of peat burning and pyroconvective injection, *J. Geophys. Res.*, *112*, D12503, doi:10.1029/2006JD007281.

Wang, T., A. J. Ding, D. R. Blake, W. Zahorowski, C. N. Poon, and Y. S. Li (2003), Chemical characterization of the boundary layer outflow of air pollution to Hong Kong during February–April 2001, *J. Geophys. Res.*, *108*(D20), 8787, doi:10.1029/2002JD003272.

Wild, O., and M. J. Prather (2006), Global tropospheric ozone modeling: quantifying errors due to grid resolution, *J. Geophys. Res.*, *111*, D11305, doi:10.1029/2005JD006605.

Wofsy, S. C., et al. (1992), Atmospheric chemistry in the Arctic and sub-Arctic: Influence of natural fires, industrial emissions, and stratospheric inputs, *J. Geophys. Res.*, *97*(D15), 16,731–16,746.

Yokelson, R. J., I. T. Bertschi, T. J. Christian, P. V. Hobbs, D. E. Ward, and W. M. Hao (2003), Trace gas measurements in nascent, aged, and cloud-processed smoke from African savanna fires by airborne Fourier transform infrared spectroscopy (AFTIR), *J. Geophys. Res.*, *108*(D13), 8478, doi:10.1029/2002JD002322.

Zhao, Y., et al. (2002), Spectroscopic measurements of tropospheric CO, C_2H_6, C_2H_2, and HCN in northern Japan, *J. Geophys. Res.*, *107*(D18), 4343, doi:10.1029/2001JD000748.

D. J. Jacob, S. Turquety, and Y. Xiao, Department of Earth and Planetary Sciences and Division of Engineering and Applied Sciences, Harvard University, Cambridge, MA, USA. (xyp@io.harvard.edu)